文章编号 2095-1531(2018)01-0131-21

Preliminary design and analysis of telescope for space gravitational wave detection

WANG Zhi[1*], SHA Wei[1], CHEN Zhe[1], KANG Yu-si[1], LUO Zi-ren[2], LI Ming[3], LI Yu-peng[1,4]

(1. *Changchun Institute of Optics, Fine Mechanics and Physics, Chinese Academy of Sciences, Changchun* 130033, *China*;
2. *Institute of Mechanics, Chinese Academy of Sciences, Beijing* 100190, *China*;
3. *DFH Satellite Co., LTD, Beijing* 100094, *China*;
4. *University of Chinese Academy of Sciences, Beijing* 100049, *China*)

* *Corresponding author, E-mail: wz*070611@126.*com*

Abstract: The direct detection of gravitational waves opens up a new era of gravitational wave astronomy, and 100-year-old prediction on gravitational wavers by Einstein have been confirmed ultimately. The space gravitational wave detector makes it possible to detect rich sources of gravitational waves in the 0.1 mHz – 1 Hz band. The space gravitational wave detector and the ground gravitational wave detector complement each other, and the combination of the two methods can realize the detection of gravitational waves in a broader band, thus uncovering more secrets of the early universe. Spatial laser interferometry gravitational wave detection uses heterodyne interferometry to measure changes in the order of 10 pm between two free-floating test masses that are millions of kilometers apart. Telescope is an important part of the laser interferometry system. Unlike the traditional geometrical imaging telescope, the telescope of the laser interferometry system shall meet the requirements of optical path stability for 1 pm and that of a harsh stray light. Based on the mission requirements of the Taiji Program in Space, this paper analyzes the functions and technical requirements of the telescope and completes the preliminary design of the principle prototype. In this paper, the sensitivity of the telescope system is analyzed according to the wavefront distribution in the far field of one million kilometers. At the same time, the thermal integration simulation in orbit is completed, which lays the technical foundation for the development of the subsequent principle prototypes.

Key words: telescope; space-based gravitational waves detection; Taiji Programe in Space; LISA; laser interferometric system

---

收稿日期: 2017-06-11; **修订日期:** 2017-08-13

基金项目: 中国科学院战略性先导科技专项(B): 多波段引力波宇宙研究——空间太极计划预研(No. XDB23030000)

Supported by Strategic Priority Research Program of the Chinese Academy of Sciences(No. XDB23030000)

空间引力波探测望远镜初步设计与分析

王 智[1*],沙 巍[1],陈 哲[1],王永宪[1],康玉思[1],罗子人[2],黎 明[3],李钰鹏[1,4]
(1. 中国科学院 长春光学精密机械与物理研究所,吉林 长春 130033;
2. 中国科学院 力学研究所,北京 100190;
3. 航天东方红卫星有限公司,北京 100094;
4. 中国科学院大学,北京 100049)

摘要: 引力波的直接观测已开启引力波天文学的新篇章,爱因斯坦的百年预言终获证实。空间引力波探测器使得探测0.1 mHz~1 Hz频段丰富的引力波源成为可能,与地面引力波探测器互为补充,才可实现更加宽广波段的引力波探测,揭开宇宙早期的更多秘密。空间激光干涉引力波探测采用外差干涉测量技术,测量间距百万公里的两自由悬浮测试质量间10 pm量级的变化量。望远镜是激光干涉测量系统的重要组成部分,1 pm的光程稳定性及苛刻的杂散光要求,不同于传统的几何成像望远镜。本文根据空间太极计划任务需求,对望远镜的功能及技术要求进行了分析,并完成了原理样机的初步方案设计,针对百万公里远场波前分布,分析了望远镜系统的敏感性,同时完成了在轨光机热集成仿真,为后面原理样机的研制奠定了技术基础。

关 键 词: 望远镜; 空间引力波探测; 空间太极计划; LISA; 激光干涉测量系统
中图分类号: TH743 **文献标识码:** A doi: 10.3788/CO.20181101.0131

1 Introduction
引 言

On February 11, 2016, the National Science Foundation announced at the National Media Center in Washington, DC that the LIGO first detected the gravitational waves created by the collision of double black holes. Gravitational wave caused by an earth-shattering collision and coalescence 1.3 billion kilometers away experienced long years of brushing the Earth which have been just caught by two upgraded LIGO detectors that just put into operation. 100-year-old prediction by Einstein finally is confirmed and mankind entered a new era of gravitational waves. Since most of the gravitational wave sources are distributed in the mHz frequency band, to detect the gravitational wave sources in this frequency band, the arm length of the interferometer must reach the order of millions of kilometers. Affected by the radius of curvature of the earth, interferometers of this magnitude can only be realized in space. The recent announcement of the amazing performance of the LISA Pathfinder validates the technical feasibility of the static control of the test mass in space, the towless control of the aircraft and the flight verification of the intra-satellite laser interferometer, thus clearing away the technical obstacles for the realization of the LISA space laser interferometer gravitational wave detector.

2016年2月11日,美国国家科学基金会在华盛顿特区国家媒体中心发布了LIGO首次探测到双黑洞碰撞产生的引力波。13亿光年外一次惊天动地的碰撞和并合激起的涟漪经历漫长的岁月掠过地球,被两台刚刚升级完毕投入运行的LIGO探测器逮个正着。爱因斯坦百年预言终于得到证实,人类进入了引力波的新纪元。由于多数的引力波源分布在mHz频段,要探测该频段的引力波源,干涉仪的臂长需达到百万公里量级。受地球曲率半径的影响,这个量级的干涉仪只有在空间才可实现。近期公布的LISA Pathfinder展示了惊人的性能:在空间验证了测试质量的静电控制、飞行器无拖曳控制的技术可行性以及星内激光干涉仪的飞行验证,为后续空间激光干涉天线

(Laser Interferometer Space Antenna,LISA) 空间激光干涉引力波探测器的实现扫清了技术上的障碍。

Spectrum of gravitational waves as a function of frequency and time. Wave sources in different frequency bands contain different physical phenomena, from quantum fluctuations in the early universe to supernova explosions and double black hole coalescence. Information contained in the coalescence of supermassive black holes, whose frequency band is in the range of 0.1 – 1 000 mHz, may reveal the formation and duration of the early structure of the universe. The process of solar-quality black hole evolved from the end of the galaxy to EMRI and the massive galaxy binary system. Gravity wave sources in different frequency bands require different means of detection. Space gravitational wave detectors require three identical satellites to form an equilateral triangle with a length of millions of kilometers [1]. The spacecraft consists of three independent Michelson interferometers with an angle of 60° and is used to measure changes in spacecraft caused by gravitational waves. The optical telescope is a key component of the space laser interferometry ranging system for the reception and emission of laser light between two spacecraft at a distance of millions of kilometers. The wavefront of the telescope system is crucial for the distribution of the intensity and the phase of the reception and emission beams. It is also important that the dimensional stability of the telescope system as part of the interference light path directly affects the range accuracy of the picometer order. This paper introduces the preliminary optical design scheme and simulation analysis of the principle prototype of telescope of the Taiji Program in Space of the Chinese Academy of Sciences, and the progress of the principle prototype.

引力波的频谱是频率和时间的函数。不同频段的波源包含不同的物理现象,从宇宙早期的量子涨落到超新星爆发以及双黑洞并合。频段在 0.1 ~ 1 000 mHz 范围,超大质量黑洞并合包含的信息可能会揭露宇宙早期结构的形成及历时,太阳质量级黑洞从星系末期演变成极大质量比黑洞绕转,以及大量的银河系双星系统。不同频段的引力波源要求不同的探测手段,空间引力波探测器需要 3 颗相同的卫星,组成边长为百万公里的等边三角形[1]。航天器间组成 3 个非独立的夹角为 60°的迈克尔逊干涉仪,用来测量由引力波引起的航天器间距的变化。而光学望远镜是空间激光干涉测距系统的关键组成部分,用来实现百万公里间距的两航天器间激光的接收和发射,望远镜系统波前对收发光束强度及相位的分布至关重要,同样重要的是作为干涉光路一部分的望远镜系统的尺寸稳定性,其将直接影响测距精度。本文介绍了中科院空间太极计划望远镜原理样机的初步光学设计方案及仿真分析,以及原理样机的进展情况。

2　Space gravitational wave detection mission
空间引力波探测任务

2.1　Mission description
任务概述

Taiji Program in Space of the Chinese Academy of Sciences mainly uses the space laser interferometry to measure the middle and low frequency gravitational waves(0.1 mHz – 1 Hz) . In addition to covering ESA´s LISA/eLISA planned detection frequency bands, this band includes sources such as coalescence of supermassive and intermediate mass black holes, EMRI system, Hanoi white dwarfs orbiting, and other cosmic gravitational radiation processes. The program focuses on the frequency range of 0.01 Hz – 1 Hz, which has a higher detection sensitivity than LISA/eLISA. Unlike the scientific goal of LISA/eLISA, the Taiji program has a significant detection advantage in focusing on intermediate mass, dual black hole orbiting systems of masses ranging from several hundred to one hundred thousand solar masses. The main scientific goal of the Taiji program is to determine the mass, spin and distribution of

black holes and the polarization of gravitational waves through the accurate measurement of gravitational waves; to explore how medium-sized seed black holes are formed; to determine whether dark matter forms a seed black hole, and how seed black holes grow into massive black holes and supermassive black holes? In addition, traces of the formation, evolution and death of the first generation of stars are investigated, direct limits on the strength of the original gravitational waves are given, direct observation data for revealing the nature of gravitation are provided.

中科院空间太极计划(Taiji Program in Space)**主要采用空间激光干涉法测量中、低频段引力波**(0.1 mHz ~ 1 Hz)。**此频段覆盖了欧空局的** LISA/eLISA **计划探测频段,其波源包括超大质量和中等质量黑洞的并合、极大质量比绕转系统、河内白矮星绕转、以及其它宇宙引力波辐射过程。太极计划探测重点在** 0.01 ~ 1 Hz **频段,具有比** LISA/eLISA **更高的探测灵敏度。另外,有别于** LISA/eLISA **的科学目标,太极计划将重点瞄准质量在几百至十万太阳质量范围内的中等质量双黑洞绕转并合系统,对此太极计划有显著的探测优势。太极计划的主要科学目标是通过精确测量引力波,测定黑洞的质量、自旋以及分布和引力波的极化; 探索中等质量种子黑洞是如何形成的,暗物质能否形成种子黑洞,种子黑洞是如何成长为大质量黑洞和超大质量黑洞的; 寻找第一代恒星形成、演化、死亡的遗迹,对原初引力波强度给出直接限制,为揭示引力本质提供直接的观测数据。**

Laser Interferometer Space Antenna(LISA) is a deep space satellite exploration mission [1] co-operated by Europe and the United States, which is mainly used to detect and study the gravitational waves at frequency band of $10^{-4} - 10^{-1}$ Hz. The basic mission concepts are described in many documents and all LISA-like mission designs use optical telescopes to send and receive beams, although the task proposals vary from country to country. The detection system adopts an equilateral triangular formation of satellites with three identical satellites at the apexes of the triangle, respectively. Each satellite contains two identical interferometer platforms, with two suspended test loads serving as the endm points of the Michelson interferometer(as shown in Fig. 1). The length of the equilateral triangle is on the order of one million kilometers and the detection of gravitational waves requires that the distance between two drag-free test masses at both ends of the measuring side should be within 10 picometers(10^{-4} to 10^{-1} Hz, arm length 5 million km). Due to the divergence angle of the Gaussian beam, the telescope's field of view and the effect of diffraction, the laser at the transmitter 2 W reaches the receiver by the order of about 100 pW. If the arm length changes, the laser emission capacity and the telescope aperture must be adjusted accordingly to ensure that the telescope in the distant spacecraft receives the same amount of energy.

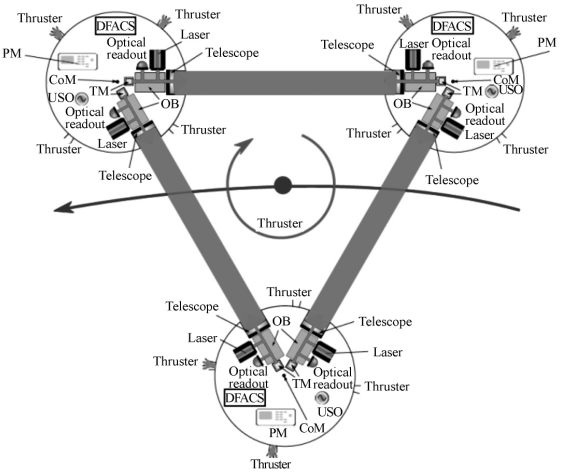

Fig. 1 A space-based gravitational wave observatory, consists of an equilateral triangle of three spacecraft with laser links between endpoint spacecraft, to measure the change in the distance between the test masses at the endpoint [3]

图1 空间引力波探测天文台,三个航天器构成等边三角形,通过端点航天器间的激光链路来测量位于端点的测试质量间距离的变化 [3]

LISA **是一个欧美合作的深空卫星探测任务** [1]**,主要是为了探测和研究频段在** 10^{-4} ~

10^{-1} Hz的引力波。基本的任务概念在很多的文献都有描述,尽管不同国家的任务建议多少有差别,但所有 LISA-like 的任务设计都使用光学望远镜来收发光束。探测系统采用等边三角形的卫星编队构型,三颗相同的卫星分别位于三角形的 3 个顶点。每颗卫星含 2 套相同的干涉仪平台、2 个悬浮的测试质量作为 Michelson 干涉仪的端点(如图 1 所示)。等边三角形的边长在百万公里量级,引力波的探测要求测量边长两端 2 个自由悬浮测试质量间距离的变化在 10 皮米量级(10^{-4} ~ 10^{-1} Hz,臂长 500 万公里)。由于高斯光束的发散角、望远镜视场以及衍射作用的影响,发射端 2 W 的激光到达接收端大约 100 pW 的量级。因此,如果臂长发生变化,发射激光能力及望远镜口径也需相应调整以保证远处航天器的望远镜接收的能量在同样的量级。

The three spacecraft of the LISA mission move in the Keplerian orbit around the sun respectively, the angle between the plane formed by the three spacecraft and the ecliptic is 60° (Fig. 2), the formation of triangles will make a complete revolution within a year while the spacecraft is spinning around

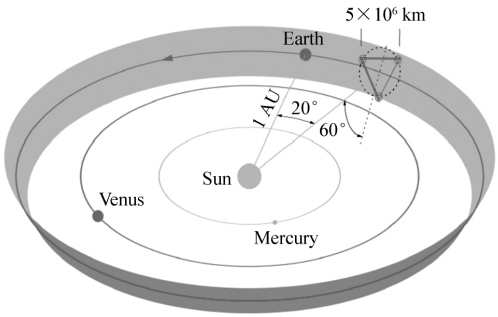

Fig. 2　Schematic diagram of LISA orbit and spacecraft formation. The angle between the spacecraft plane and the ecliptic plane is about 60°. The constellation trails earth by about 20°, and the distance between spacecraft is 5×10^6 km[3]

图 2　LISA 轨道及航天器编队示意图,航天器组成的平面与黄道面夹角约为 60°,航天器星座质心落后地球约 20°,航天器之间的距离为 5×10^6 km[3]

the Sun. LISA´s orbital design is the simplest and the most mature design, and the configuration of the three spacecraft ensures that the mission will be in stable operation for five years, and even up to 8 years.

LISA 任务的 3 个航天器各自运行在开普勒轨道绕日飞行,3 个航天器构成的平面与黄道面夹角为 60°(图 2),航天器在绕日转动的同时三角形队形在一年内会转动一周。LISA 的轨道设计是最简单也是最成熟的,3 个航天器的构型可以使任务在轨稳定运行 5 年,甚至可达到 8 年。

2.2　Measuring principle
测量原理

In the theory of relativity, the influence of gravitational waves passes upon space-time can be regarded as the perturbation in the flat space-time background. The influence of gravitational waves on the triangular configuration of the LISA-like spacecraft is shown in Fig. 3, where "+" and "×" are two independent polarization directions of the gravity wave. The propagation of photons or other matter particles in time and space can be described by the metric line elements. When the gravitational waves pass through the space-time, the space-time metric tensor changes, resulting in changes in the propagation state of particles such as photons. At the same time, changes of the metric tensor will cause changes in space-time curvature, and then change the level of tidal forces between two points in space-time.

在相对论中,引力波经过时对时空的影响可以看成平直时空背景下的微扰,引力波对 LISA-like航天器三角形构型的影响如图 3 所示,其中,"+"和"×"为引力波两个独立的偏振方向。光子或其他物质粒子在时空中的传播可以用度规线元来刻画,当引力波经过该时空时,其时空度规张量发生改变,引起光子等物质粒子的传播状态发生变化;同时,度规张量改变还会引起时空曲率发生变化,继而改变该时空中两点间潮汐力的大小。

Based on the above principle, the space gravi-

tational wave detector uses the free-floating test mass as a sensor, and adopts heterodyne laser interferometry to obtain small changes caused by the space-time structure when the gravitational wave passes through. For convenience, we only consider one polarization direction "+" when the gravitational wave propagates. Without considering the effects of gravitational waves($\bar{h}_+ = 0$) , the time for light to travel back and forth between two test masses is [4-5]

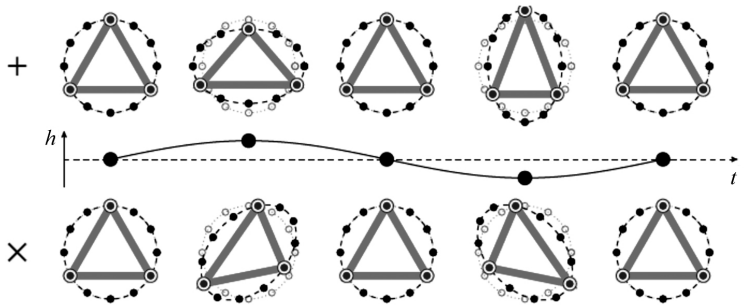

Fig. 3 Gravity waves pass through the triangle formation formed by the test masses. The three test masses in formation represent three LISA spacecraft, the time variable of the red arm length represents the distance variation caused by the gravitational wave that needs to be measured

图 3 引力波经过测试质量组成的三角形编队。三角形编队中 3 个测试质量代表 3 个 LISA 航天器,红色臂长的时变量即需要测量的引力波引起的距离变化量 [1]

空间引力波探测器正是基于上述原理,利用自由悬浮的测试质量作为传感器,采用外差激光干涉测量的方法来获得当引力波经过时时空结构所产生的微小变化。考虑叙述方便,只考虑引力波传播时的一个偏振方向"+"。不考虑引力波影响时($\bar{h}_+ = 0$) ,光在两个测试质量间往返一次的时间如公式(1) 所示 [4-5] **。**

$$t_2 - t_0 = \frac{L}{c}\ , \qquad (1)$$

In equation (1) , L is the distance $|x_1 - x_2|$ between two test masses. When the gravitational wave passes through the space-time, the round-trip time of the light between the two test masses will change. The relationship between the amount of time change and the amplitude of the gravitational wave is

式中,L 为两测试质量之间的距离 $|x_1 - x_2|$。当引力波经过该时空时,光在两测试质量间的往返时间会发生改变,时间改变量 Δt 与引力波振幅的关系如公式(2) :

$$\Delta t = \frac{1}{c} L\bar{h}_+ . \qquad (2)$$

The amount of change in distance caused by the amount of time change is:

由该时间改变量引起的距离变化量如公式(3) :

$$c\Delta t = L\bar{h}_+ . \qquad (3)$$

Assuming an orbiting system consists of two black holes with a mass of one hundred thousand solar masses, the gravitational wave intensity h is on the order of 10^{-13} when gravitational radiation released by the orbiting system is in the frequency band of 1 mHz. If the orbiting system is 400 million light-years from the earth, the intensity h is about 10^{-21} when gravitational waves propagate to the earth. If the two test masses are 5×10^6 km apart, the distance between the test masses caused by the gravitational waves is in the order of 10 pm.

假设有一绕转系统是由两个十万太阳质量的黑洞构成,绕转系统释放的引力辐射在 1 mHz 频段时,引力波的强度 h 为 10^{-13}量级。如果该绕转系统距离地球为 4 亿光年,当引力波传播到地球,强度 h 约变为 10^{-21}。若两测试质量相距 5×10^6 km,则由引力波引起的测试质量间距离变化量约为 10 pm 量级。

2.3 Telescope function
望远镜的功能

There are two main functions of the telescope in the laser interferometry ranging system: one is to expand the small-diameter beam used in the interference optical platform to a collimated beam close to the diffraction limit; the other is to enable the interferometric laser beam to be efficiently transmitted between the two spacecraft and to receive the incident beam from the far-end spacecrafts while emitting the beam. Fig. 4 shows the concept maps of LISA interferometry system and that of binary satellite interferometry, from which the effect of the telescope can be found. The laser light is emitted from spacecraft 1, expanded by a telescope, and propagated to a spacecraft 2 of 5×10^6 km. Only a small portion of the light energy can be received by the far-end telescope. Fig. 5 shows one of the optical payload systems on the spacecraft [6-13].

激光干涉测距系统中的望远镜的主要功能有两个: 一是将干涉光学平台用的小直径光束扩束成接近衍射极限的准直光束; 二是使干涉测量用激光束在两个航天器间有效的传输,发射光束的同时接收来自远端航天器的入射光束。图 4 表示的是 LISA 干涉测量系统概念图以及双星干涉测量概念图,图中可以看出望远镜的作用。激光从

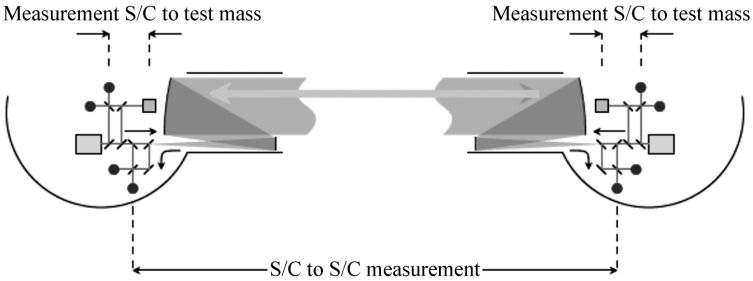

Fig. 4　The functions of the telescope is to send and receive laser beams efficiently between the two spacecraft and to establish a laser link for the precise measurement of the change in the distance between the two test masses [7]

图 4　望远镜的功能,在两航天器间有效的收发激光束,建立激光链路用于精密测量两测试质量间距离的变化 [7]

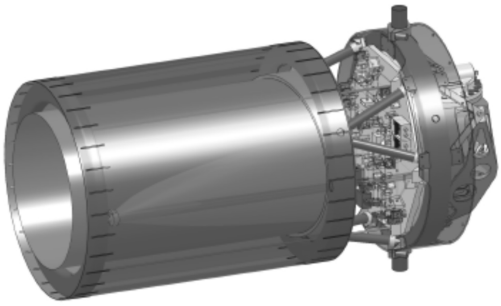

Fig. 5　LISA optical load model, the interferometer telescope optical axis is perpendicular to the interferometer optical platform. The test masses are fixed behind the optical platform [8]

图 5　LISA 光学载荷模型,望远镜视轴与干涉仪光学平台垂直,测试质量固定在光学平台后面 [8]

航天器 1 发出,经望远镜扩束后,传播到 5×10^6 km的航天器 2,只有很少一部分光能被远端望远镜接收。图 5 为航天器上其中的一个光学有效载荷系统 [6-13]。

Assuming that the laser power emitted by the telescope of spacecraft 1 is P_0, the laser power received by the spacecraft 2 telescope will be P, when the laser power is propagated to the remote spacecraft 2. The laser waist is designed at telescope exit pupil, and the waist size should be the same as the size of the exit pupil of the telescope, then we obtain

假设航天器 1 望远镜发出的激光功率为 P_0, 传播至远端的航天器 2 时,航天器 2 望远镜接收到的激光功率为 P。将激光的束腰设计在望远镜出瞳处,并且束腰大小与望远镜出瞳尺寸一致,则有公式(4)。

$$P = \frac{1}{2}\frac{D^4}{\lambda^2 L^2}P_0, \tag{4}$$

Where D is the telescope aperture, L is the distance between two spacecrafts, λ is the laser wavelength. For LISA missions, $\frac{P}{P_0}<10^{-10}$. LISA is currently planning to use a laser with a power of 2 W and a remote spacecraft 2 telescope with a laser power of the order of 100 pW. This order of light can not be returned directly to spacecraft 1 for measurement. Therefore, the working mode of space gravitational wave detection is different from that of the ground gravitational wave detector, weak-light phase-locking amplification technology must be adopted. A hundred picowatt-order laser received by remote spacecraft 2 interferes with the local laser, the phase difference information is derived from the interference signal, the phase of the local laser is locked to the received phase of the laser, and then the phase locked local laser is retransmitted back to the spacecraft 1. The laser intensity received by the spacecraft 1 telescope is also on the order of hundred picowatt and its phase information is maintained.

式中，D 为望远镜口径，L 为两航天器之间的距离，λ 是激光波长。对于 LISA 任务要求，$\frac{P}{P_0}<10^{-10}$。LISA 目前计划使用的激光器功率为 2 W，此时远端航天器 2 望远镜接收到的激光功率约为 100 pW 量级。由于这个量级的光无法直接返回航天器 1 进行测量。所以，空间引力波探测的工作方式不同于地面引力波探测器，必须采用弱光锁相放大技术，使远端航天器 2 接收到的百皮瓦量级激光与本地激光进行干涉，从干涉信号解出相位差信息，将本地激光器的相位锁定在接收到的激光相位，然后将锁定相位后的本地激光再发射回航天器 1。航天器 1 望远镜接收到的激光光强同样在百皮瓦量级，并且其相位信息得以保持。

It can be seen from Fig. 4 that the interferometric measurement of the space gravitational wave detection task is jointly implemented by three parts: one is the interference measurement of the change in the distance between the spacecraft 1 and the test mass 1; the other is the interferometric measurement of the change of the distance between the spacecraft 1 and the spacecraft 2; and the third is the interferometric measurement of the change in the distance between spacecraft 2 and test mass 2. Spacecraft 1 and spacecraft 2 are equipped with independent lasers, denoted as $E_1\cos(\omega_1 t+\varphi_1)$ and $E_2\cos(\omega_2 t+\varphi_2)$ respectively. After being received by the spacecraft 2 telescope, the spacecraft 1 emits a laser beam to interfere with the local laser to generate an interference signal $E\cos(\Delta\omega t+\Delta\varphi)$, where $\Delta\varphi=(\varphi_1-\varphi_2)+\frac{2\pi}{\lambda}(l_1+L+2L_R-l'_1)$. The phase difference information between the received light and the local laser is obtained from the interference signal and fed back to the light source controller of the spacecraft 2. The phase of the laser light of the spacecraft 2 is locked with the phase of the received light and the local laser of the spacecraft 2 is:

由图 4 可以看出，空间引力波探测任务的干涉测量由 3 部分共同实现：第 1 部份是航天器 1 与测试质量 1 之间距离变化的干涉测量；第 2 部份是航天器 1 与航天器 2 之间距离变化的干涉测量；第 3 部份是航天器 2 与测试质量 2 之间距离变化的干涉测量。航天器 1 和航天器 2 均装有独立的激光器，分别表示为 $E_1\cos(\omega_1 t+\varphi_1)$ 和 $E_2\cos(\omega_2 t+\varphi_2)$。由航天器 2 望远镜接收到航天器 1 望远镜发射来的激光后，与本地激光发生干涉，产生干涉信号 $E\cos(\Delta\omega t+\Delta\varphi)$，其中 $\Delta\varphi=(\varphi_1-\varphi_2)+\frac{2\pi}{\lambda}(l_1+L+2L_R-l'_1)$。从干涉信号里解出接收光与本地激光的相位差信息，反馈给航天器 2 的光源控制器，将航天器 2 激光的相位跟接收光的相位锁定，航天器 2 本地激光变为：

$$E_2\cos(\omega_2 t+\phi_2+\Delta\phi)=E_2\cos\left[\omega_2 t+\phi_1+\frac{2\pi}{\lambda}(l_1+L+2L_R+l'_1)\right]. \tag{5}$$

Laser after phase-locked on the spacecraft 2 is emitted back to the spacecraft 1, it interferes with the local laser on the spacecraft 1 after being reflected by the test mass of the spacecraft 1 to generate an interference signal $\cos\left[\Delta\omega t+\frac{2\pi}{\lambda}(2L+2L_R+\right.$

$2L_1)]$. It can be seen that the phase of the interference signal contains information about the distance between the test masses.

将航天器 2 上锁相后的激光发射回航天器 1,经航天器 1 测试质量反射后与航天器 1 上的本地激光发生干涉,产生干涉信号 $\cos\left[\Delta\omega t+\frac{2\pi}{\lambda}(2L+2L_R+2L_L)\right]$。可见,在此干涉信号的相位中包含了测试质量间距离的信息。

3　Design and analysis of telescopic optical system
望远镜光学系统设计与分析

3.1　Technology requirements of system-level telescope
系统级望远镜技术要求

Table 1 shows the key technical indicators of the principle prototype of the telescope in Taiji Program in Space(refer to the eLISA task) . The principle prototype of the telescope is used as the design input according to this[6-13]. The same design considerations also apply to other LISA-like tasks, and this paper discusses only the technical requirements that affect the design of the optical system and other important factors.

Tab. 1　Key technology requirements of telescope
表 1　望远镜关键技术指标

Characteristics	Requirements
Aperture	20 cm
Optical efficiency	≥0.853
Field of view	
acquisition mode	400 μrad full angle
Science mode(out of plane)	±7 μrad
(in plane)	±4.2 μrad in-plane
Optical path length stability	$1\frac{\text{pm}}{\sqrt{\text{Hz}}}\times\sqrt{1+\left(\frac{3\text{ mHz}}{f}\right)^4}$
Magnification	40
Far-field wavefront quality	λ/20

表 1 为太极计划望远镜原理样机的关键技术指标(参考 eLISA 任务) ,望远镜原理样机根据此作为设计输入[6-13]。相同的设计考虑同样适用于其它的 LISA-like 任务,本文仅就影响光学系统设计以及涉及其它重要因素的技术要求进行简单讨论。

The choice of the working band of the telescope is determined by the laser used by the space gravitational wave detector. Taiji program plans to run in orbit for 5 years, the laser should have good frequency stability, phase stability and power stability, and should meet the needs of high-power and space working environment. Through comprehensive consideration, we decided to adopt the relatively mature 1 064 nm Nd:YAG solid state laser.

望远镜工作波段的选择是由空间引力波探测器使用的激光器决定的。太极计划拟在轨运行 5 年,激光器需要有很好的频率稳定性、相位稳定性和功率稳定性,并且尽量满足大功率以及空间工作环境的需求。综合考虑,计划采用技术相对成熟的 1 064 nm Nd:YAG 固体激光器。

(1) Far-field system wavefront
远场系统波前

Due to the presence of respiration angles between spacecrafts, the boresight between the two spacecraft telescopes will jitter, and this jitter will be directly coupled into a TTL(Tilt-To-Length coupling) , which is the main source of noise other than shot noise. To minimize the TTL, center the telescope´s outgoing wavefront at the spacecraft´s center of mass, with far field spherical wave and as smooth as possible. Such TTL noise will not be introduced when the spacecraft is jittered along the telescope´s visual axis due to the uniform radii of the spherical wavefront in all directions. However, if there are aberrations in the telescope system, such as the first three aberrations(Piston, Tilt x, Tilt y) , the far-field wavefront pointing at millions of kilometers will jitter and then TTL noise will be introduced(the contribution of telescopes to the TTL interferometry system, this topic will be elaborated in another paper) . Although this error term associated with

spacecraft pointing can partly eliminated by the alignment between spacecraft, the most effective way to minimize the TTL noise generated by the telescope is to design the wavefront near the diffraction limit.

由于航天器之间呼吸角的存在,两航天器望远镜之间的视轴会发生抖动,这个抖动将直接耦合成为 TTL(tilt-to-length coupling) 噪声,它是除散粒噪声之外最主要的噪声源。为了尽量减小 TTL,使望远镜出射波前的中心位于航天器的质心,远场为球面且尽量光滑。这样当航天器沿望远镜视轴方向抖动时,由于球面波前所有方向半径一致,故不会引入此类 TTL 噪声。而如果望远镜系统存在像差,如像差前三项(Piston,Tilt x,Tilt y) ,则在百万公里处的远场波前指向就会产生抖动,继而引入 TTL 噪声(望远镜对干涉测量系统 TTL 的贡献,该工作正在开展,拟另文详述) 。尽管这个与航天器指向有关的误差项可以通过航天器之间的对准消除一部分,但最有效的方法是通过设计接近衍射极限的波前来尽量减小望远镜产生的 TTL 噪声。

Another reason why telescopes require high wavefront quality is to maximize the transmission efficiency of beam energy between the two spacecrafts. The Strehl ratio is usually adopted as a criterion for this feature. In the interfering arm of the space gravitational wave detection system, there are two telescope systems, which are respectively responsible for transmitting and receiving, and the beam energy transmission efficiency is proportional to the square of the Strehl ratio. If the system wavefront error of the single-link measurement is $\sigma = \lambda/20$, the corresponding Strehl ratio is: $1 - (2\pi\sigma)^2 = 0.9$. Therefore, if two sets of telescope systems for transmitting and receiving are considered, the beam energy transfer efficiency is proportional to $0.9^2 = 0.8$, which can be used as a criterion for the diffraction limit of the optical system. Considering that there must be aberrations in the optical components on the interferometric optical platform, while leaving a certain margin for the assembly of the interferometer optical system, the permissible wavefront error of the telescope system is $\lambda/30$.

要求望远镜具有高的波前质量的另一个原因是: 尽量提高两航天器间光束能量的传输效率。通常使用斯特列尔比(Strehl ratio) 作为该特性的质量评价指标,在空间引力波探测系统的干涉臂中有发射和接收两套望远镜系统,其光束能量传输效率与斯特列尔比的平方成正比。如果单链路测量的系统波前误差为 $\sigma = \lambda/20$,则对应的斯特列尔比为: $1 - (2\pi\sigma)^2 = 0.9$。考虑到收发为两套望远镜系统,故光束能量传输效率应与 $0.9^2 = 0.8$ 成正比,且作为光学系统衍射极限的判据。考虑干涉光学平台上光学元件一定会存在像差,同时为干涉仪光学系统的装配留有一定的裕量,本文要求望远镜系统的波前误差为 $\lambda/30$。

(2) Optical transmission efficiency

光学传输效率

Telescope transmission efficiency is determined by the shot noise of the telescope system. The shot noise of the system is also one of the most important noise sources in the laser interferometry system. This noise is mainly due to the fluctuation of photon number, and the fluctuation of photon number follows Poisson statistics. If the laser power is P, the number of photons per unit time can be expressed as $N = \frac{P}{h\nu}$, and the number of fluctuations in the number of photons follows Poisson statistics, which can be expressed as:

望远镜的传输效率是由望远镜系统的散粒噪声决定的。系统的散粒噪声同时也是激光干涉测量系统最主要的噪声源之一,产生原因主要是光子数的涨落,且光子数的涨落服从泊松统计。如果激光的功率为 P,单位时间内的光子数可以表示为 $N = \frac{P}{h\nu}$,光子数的涨落服从泊松统计,可表示公式(6) :

$$\Delta N = \sqrt{N} = \sqrt{\frac{P}{h\nu}}, \tag{6}$$

According to the uncertainty principle of quantum mechanics, the phase fluctuation of laser $\Delta\varphi$

and photon number fluctuation ΔN have the following relations:

根据量子力学测不准原理,激光的相位涨落 $\Delta\varphi$ 与光子数涨落 ΔN 存在如式(7)关系。

$$\Delta\varphi\Delta N \geqslant 1 . \tag{7}$$

There is a conversion relationship $\delta_1 = \frac{\lambda}{2\pi} \cdot \Delta\varphi$ between distance variation δ_1 and phase variation, thus we get the expression of shot noise as follows:

距离变化量 δ_1 与相位变化量 $\Delta\varphi$ 存在转换关系 $\delta_1 = \frac{\lambda}{2\pi} \cdot \Delta\varphi$,由此可以得出散粒噪声的表达式如式(8)。

$$\delta_1 = \sqrt{\frac{hc\lambda}{2\pi P}} . \tag{8}$$

If the spacecraft 1 telescope emits laser power P_0, the exiting light is TEM_{00} mode Gaussian beam. In order to reduce the divergence of the beam, it is necessary to increase the beam waist of the outgoing beam ω, for the case of LISA, $\omega = 0.446D$, D is taken as the aperture of the telescope system. Then at a distance of 5×10^6 km from spacecraft 1 telescope, the laser power that telescope of spacecraft 2 can receive is calculated by equation (4).

如果航天器 1 的望远镜发出的激光功率为 P_0,出射光为 TEM_{00} 模的高斯光束。为了减小光束的发散,需增大出射光束的束腰 ω,LISA 取 $\omega = 0.446D$,D 为望远镜系统口径。那么在距离航天器 1 的望远镜 5×10^6 km 处,航天器 2 的望远镜能接收到的激光功率见式(4)。

Taking into account the losses caused by optical components when the laser propagates in the interferometer, the actual received light intensity from the spacecraft 2 telescope will be lower. Let the total optical efficiency of the entire laser interferometry system be ε, and the optical efficiency given by LISA is $\varepsilon \approx 0.3$. If the laser light intensity emitted by the spacecraft 1 telescope is 2 W, the wavelength is 1 064 nm and the telescope aperture is 400 mm, the shot noise of the laser interferometry system is $\delta_1 = 1 \times 10^{-11}\,\mathrm{m}/\sqrt{\mathrm{Hz}}$.

考虑到激光在干涉仪中传播时由光学元件产生的损耗,航天器 2 望远镜实际接收到的光强会更低,设整个激光干涉测量系统的总光学效率为 ε,参考 LISA 给出的光学效率 $\varepsilon \approx 0.3$。如果航天器 1 望远镜发射的激光光强为 2 W,波长为 1 064 nm,望远镜口径为 400 mm,则激光干涉测量系统的散粒噪声为: $\delta_1 = 1 \times 10^{-11}\,\mathrm{m}/\sqrt{\mathrm{Hz}}$。

Shot noise is the intrinsic noise of an interferometric system. From the previous analysis it can be concluded that this noise can only be reduced by increasing the telescope aperture or increasing the laser power. In determining the telescope aperture and emitting laser power, if the shot noise is to be reduced, only the light intensity received by the spacecraft 2 can be increased, that is, the energy transfer efficiency of the optical system can only be increased as much as possible. For four-mirror system used in the prototype telescopes, a technical index of >0.853 requires that the reflectance of each mirror be better than 0.96, but stray light specifications may require a higher reflectance of the mirror.

散粒噪声是干涉测量系统的内禀噪声,从前面的分析可以得出,该噪声只能通过增大望远镜口径或增大激光器功率来减小。在望远镜口径以及发射激光器功率确定的情况下,要降低散粒噪声,只能增大航天器 2 接收到的光强,也就是说只能尽量提高光学系统的能量传输效率。对于望远镜原理样机采用的四反系统,>0.853 的技术指标要求每个反射镜的反射率优于 0.96,但杂散光的技术指标会要求反射镜的反射率更高。

(3) Field of view

视场

Telescope´s field of view is divided into science and acquisition field of view.

望远镜的视场分为科学视场和捕获视场。

The scientific field of view of telescopes is the range of field of view required by the telescope in scientific measurement. The selection of the arm length and orbit of the interferometric system determines the instantaneous field of view of the tele-

scope. As each spacecraft turns around the sun in its own orbit, the launched telescope should consider the location of the receiving telescope in advance due to millions of kilometers of arm length and limited speed of light to ensure initial inter-satellite alignment. The scientific field of view of the telescope is determined from the orbital stability index of the advance pointing angle.

望远镜科学视场指的是在科学测量过程中，望远镜可以保证的视场角范围。干涉测量系统臂长及轨道的选择就确定了望远镜的瞬时视场。当每个航天器在各自轨道绕日转动时，由于几百万公里的臂长以及有限的光速，发射望远镜需要提前指向接收望远镜的位置，以确保实现初步星间对准。根据轨道给出的提前指向角度的稳定性指标，来确定望远镜的科学视场角。

Interferometric measurements of changes in the distance between two spacecrafts require that the inter-satellite laser link be established by the telescope first. Since the capture between the spacecraft is open-loop, the capture field of view of the telescope is determined based on the selected arm length and orbit and the acquisition strategy angle.

对于两航天器间距离变化的干涉测量，需要首先通过望远镜建立星间激光链路，由于航天器间的捕获是开环的，所以可根据选取的臂长及轨道，以及捕获策略，确定望远镜的捕获视场角。

(4) Optical length stability

光程稳定性

The optical path stability of the telescope is determined by the allocation of noise budget of the single-link measurement system, which varies from one spacecraft to another, to the telescope subsystem. The total noise budget of the single link measurement system is

望远镜的光程稳定性要求是由两测量航天器间距离变化的单链路测量系统噪声预算分配给望远镜子系统确定下来的。单链路测量系统总的噪声预算(NB)如式(9)。

$$\mathrm{NB} = 12 \times \frac{\mathrm{pm}}{\sqrt{\mathrm{Hz}}} \times \sqrt{1 + \left(\frac{f_0}{f}\right)^4}, \quad (9)$$

$0.1\ \mathrm{mHz} \leqslant f \leqslant 1\ \mathrm{Hz}, f_0 = 2.8\ \mathrm{mHz}$.

Noise of the optical path stability distributed by the telescope system is $1\ \mathrm{pm}/\sqrt{\mathrm{Hz}}$, $0.1\ \mathrm{mHz} \leqslant f \leqslant 1\ \mathrm{Hz}$.

而望远镜系统分配的光程稳定性噪声为 $1\ \mathrm{pm}/\sqrt{\mathrm{Hz}}$, $0.1\ \mathrm{mHz} \leqslant f \leqslant 1\ \mathrm{Hz}$。

3.2 Telescope optical system design

望远镜光学系统设计

According to the technical requirements of the telescope principle prototype(see Tab. 1), and the functions and effects of the telescopes analyzed in the previous section, and considering the harsh stray light requirements, the initial program of the telescope optical system adopts the structure of the off-axis and four-mirror(as shown in Fig. 6) [6-13]. The main mirror M1 is an off-axis paraboloidal mirror, the secondary mirror M2 is an off-axis hyperbolic mirror, the rear third mirror M3 and the fourth mirror M4 are spherical. An image plane is designed between M2 and M3. Setting an liminayinh stray light stop at this position effectively suppresses stray light. M3, M4 components can be adjusted when the telescopeis in orbit to compensate the vibration due to satellite launch, orbit transfer and system wavefront quality worsening due to changes in the structure parameters of the telescope caused by stress release and temperature gradient in micro gravity after entering orbit.

根据望远镜原理样机的技术要求(见表1)，结合前面对望远镜的功能及作用分析，考虑苛刻的杂散光要求，望远镜光学系统初步方案采用离轴四反的结构形式(如图6所示)[6-13]。主镜M1是离轴抛物面，次镜M2为离轴双曲面，后组三镜M3和四镜M4均为球面。光学系统在M2和M3之间设计有一次像面，在此位置设置消杂光光阑可以有效抑制杂散光。望远镜入轨后可以调节M3、M4组件，以补偿由于卫星发射、变轨带来的振动，以及入轨后微重力环境下的应力释放、温度梯度造成的望远镜结构参数变化导致的系统波前质量下降。

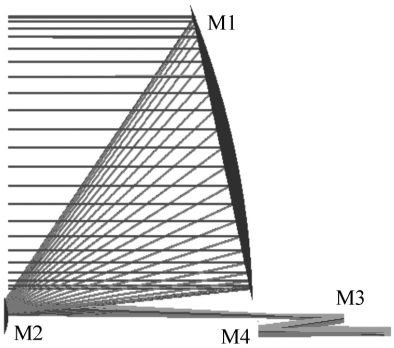

Fig. 6　Optical system design of telescope

图 6　望远镜光学系统设计

From the analysis of 2.1, we can see that the telescope has a very good wavefront quality whether it is to minimize the TTL noise or to improve the energy transmission efficiency of interferometric link beam. Fig. 7 shows the wavefront error at the exit pupil of the system, with an RMS value of 0.013λ.

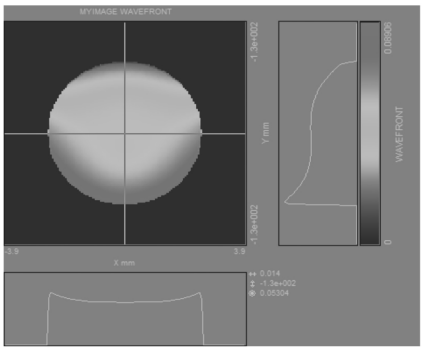

Fig. 7　Wavefront performance at exit-pupil of telescope, RMS is 0.013λ

图 7　系统出瞳处波前质量,RMS 值 0.013λ

Fig. 8 and Fig. 9 show the intensity distribution and phase distribution at the exit pupil.

由 2.1 节的分析可知,无论是尽量减少 TTL 噪声,还是尽量提高干涉测量链路光束能量传输效率,都要求望远镜具有非常好的波前质量。图 7 为系统出瞳处波前误差,RMS 值 0.013λ,图 8、图 9 分别为出瞳处强度分布和相位分布。

3.3　Far-field wavefront and sensitivity analysis 远场波前及灵敏度分析

From Fig. 4 and above, it can be concluded

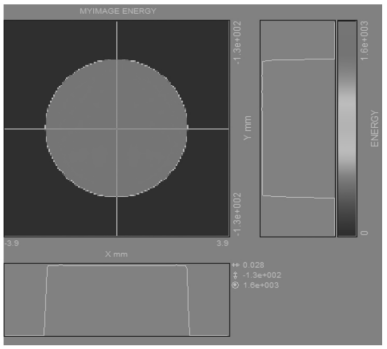

Fig. 8　Intensity distribution at exit-pupil of telescope

图 8　系统出瞳处强度分布

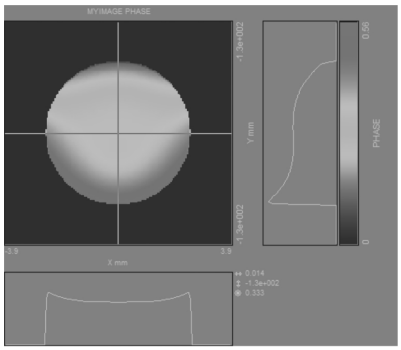

Fig. 9　Phase distribution at exit-pupil of telescope

图 9　系统出瞳处相位分布

that the LISA mission needs to measure the variation of 10 pm over a distance of 5×10^6 km. For space gravitational wave detection, LISA program consists of three spacecrafts with two telescopes on each spacecraft, thus a total of six sets of identical telescope systems. Many factors affect the interferometric measurement of the order of the picometer. Here, we mainly analyze the influence of the change of structural parameters of the telescope on the far-field phase. In this case, it is assumed that the telescope acts as a beam expander transmitting system (in practice, receiving and emitting are performed simultaneously).

从图 4 以及前面所述可知,LISA 任务需要测量 5×10^6 km 距离上 10 pm 的变化量。为了实现空间引力波探测,LISA 计划由 3 个航天器组成,每个航天器上有两套望远镜,一共 6 套相同的望远镜系统。许多因素会影响皮米量级的干涉测

量，这里主要分析望远镜结构参数变化对远场相位的影响，此时，假设望远镜作为扩束发射系统（实际工作时，接收和发射同时发生）。

(1) Calculation method

计算方法

In the space gravitational wave detection mission, the laser is emitted from the spacecraft 1 telescope and received by the far-end spacecraft 2 telescope. The wavefront distribution can be obtained based on Kirchhoff's diffraction formula [14]:

在空间引力波探测任务中，从航天器 1 望远镜发射激光，由远端航天器 2 望远镜接收，其波前分布可以依据基尔霍夫衍射公式确定[14]，如式(10)。

$$E(x_1,y_1) = \frac{1}{i\lambda}\int_s \frac{1}{r}E(x,y)\,e^{ikr}K(\theta)\,\mathrm{d}S\ , \tag{10}$$

Where $E(x,y)$ is the wavefront distribution of the outgoing laser at the exit pupil of the spacecraft 1 telescope, $E(x_1,y_1)$ is the wavefront distribution of the laser propagating to the far spacecraft 2 telescope, point (x,y) is any point on the S surface, (x_1,y_1) is any point on the S′ plane, r is the distance from point (x,y) to point (x_1,y_1), and $k(\theta)$ is the tilt factor. Fig. 10 is the laser wavefront propagation diagram.

式中，$E(x,y)$ 是发射激光在航天器 1 望远镜出瞳的波前分布，$E(x_1,y_1)$ 是激光传播到远端航任意一点，点 (x_1,y_1) 是 S′面上任意一点，r 是点 (x,y) 到点 $C(x_1,y_1)$ 的距离，$k(\theta)$ 是倾斜因子。激光波前传播示意图见图 10。

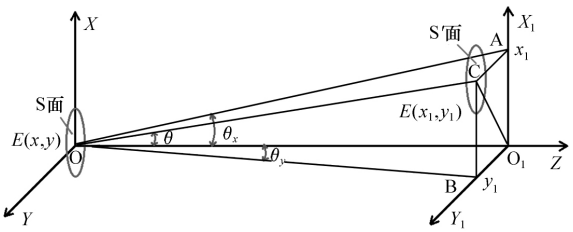

Fig. 10 Schematic diagram of wavefront propagation of laser

图 10 激光波前传播示意图

As shown in the figure, the transmitting telescope in spacecraft and the receiving telescope spacecraft are respectively in the S- and S′-planes, the X- and Y-axis are respectively parallel to the X_1- and Y_1-axes, the Z-axis represents the propagation direction of the laser light, and OC is the line of center of transmitting and receiving telescopes, the distance between OC is u. In equation (10),

图中，航天器 1 发射望远镜和航天器 2 接收望远镜分别在 S 和 S′面内，X、Y 轴分别与 X_1、Y_1 轴平行，Z 轴为激光的传播方向，OC 是发射、接收望远镜中心连线，OC 间距离为 u。式(10)中，

$$r = \sqrt{OO_1^2 + (x_1 - x)^2 + (y_1 - y)^2}$$

$$u = \sqrt{OO_1^2 + x_1^2 + y_1^2}。$$

According to the above equation, based on the

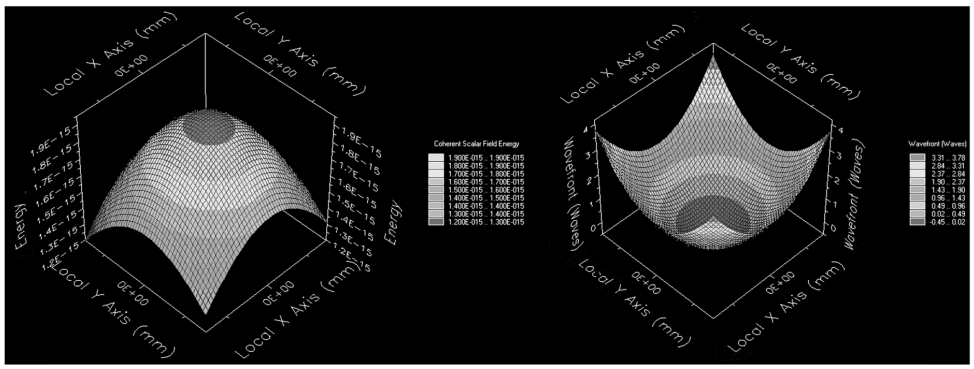

(a) Intensity distribution (b) Wavefront distribution

(a) 强度分布 (b) 波前分布

Fig. 11 Diagrams of intensity and wavefront distributions at 5×10^6 km with telescope wave front of $\lambda/60$

图 11 发射望远镜波前 $\lambda/60$，5×10^6 km 处强度(a)和波前(b)分布图

aperture of the telescope, the wavefront deformation caused by the first three terms of the Zernike polynomials is mainly considered. At the distance of 5×10^6 km, the intensity distribution and the wavefront in the far field are as shown in Fig. 11.

由上述计算方法,根据望远镜口径,主要考虑泽尼克多项式前三项引起的波前变形,5×10^6 km 处,远场的强度分布和波前如图 11 所示。

(2) Far-field wavefront sensitivity analysis

远场波前灵敏度分析

Tab. 2 shows the variation of the structural parameters of the telescope given by the reference error. Tab. 3 shows the PV value of the far-field wavefront at 5×10^6 km, and Fig. 12 – Fig. 19 show the far-field wavefront distribution and variation (As a result of length reason, only the data of most influential secondary mirror is listed here).

表 2 为参考误差允许的望远镜结构参数的变化量,表 3 为 5×10^6 km 处远场波前的变化 PV 值,图 12 ~ 图 19 为远场波前分布及变化图(篇幅原因,仅列出影响最大的次镜部分)。

Due to the change in the structural parameters of the telescope system is small, it can be considered that the variation of the structural parameters of the telescope is linear with the variation of the far-field wavefront. Considering that the expected LISA-like orbital temperature stability is on the order of 10^{-5} K, the analysis results of Fig. 12 – Fig. 19 and Tab. 3 indicate that the variation of the far-field wavefront under the structural parameters of the telescope system can meet the requirements of the space gravity wave detection.

由于望远镜系统结构参数的变化量很小,可以认为系统结构参数变化量与远场波前变化量成线性关系。考虑 LISA-like 计划要求轨道温度稳定性在 10^{-5} K 量级,由图 12 ~ 图 19 和表 3 的分析结果可知,望远镜系统结构参数失调下远场波前的变化可以满足空间引力波探测的要求。

Tab. 2　Variations of telescope parameters

表 2　望远镜结构参数变化量

Type of variations	Variations	M1	M2	M3	M4
position	X decenter/μm	0.5	0.5	0.5	0.5
	Y decenter/μm	0.5	0.5	0.5	0.5
	Z decenter/μm	0.5	0.5	0.5	0.5
	X tilt/(″)	0.4	0.4	0.4	0.4
	Y tilt/(″)	0.2	0.4	0.4	0.4
	Z tilt/(″)	0.4	0.4	–	–
surface	Radius/μm	1	1	1	1
	Conic	0.00001	0.001	–	–

Tab. 3　Far field wavefront variations(PV) at 5×10^6 km

表 3　5×10^6 km 处远场波前变化量 PV 值

Type of variations	Variations	Variation PV(λ)			
		M1	M2	M3	M4
position	X decenter/μm	8.26×10^{-6}	1.12×10^{-6}	1.33×10^{-6}	1.47×10^{-6}
	Y decenter/μm	4.34×10^{-7}	5.35×10^{-8}	1.05×10^{-7}	2.93×10^{-6}
	Z decenter/μm	4.04×10^{-7}	1.47×10^{-6}	1.31×10^{-7}	2.70×10^{-8}
	X tilt/(″)	3.33×10^{-6}	1.31×10^{-6}	1.10×10^{-6}	6.16×10^{-7}
	Y tilt/(″)	2.42×10^{-7}	5.91×10^{-8}	7.94×10^{-7}	6.61×10^{-8}
	Z tilt/(″)	3.46×10^{-9}	1.30×10^{-6}	–	–
surface	Radius/mm	8.86×10^{-7}	1.87×10^{-6}	1.26×10^{-7}	1.99×10^{-8}
	Conic	4.07×10^{-7}	1.06×10^{-6}	–	–

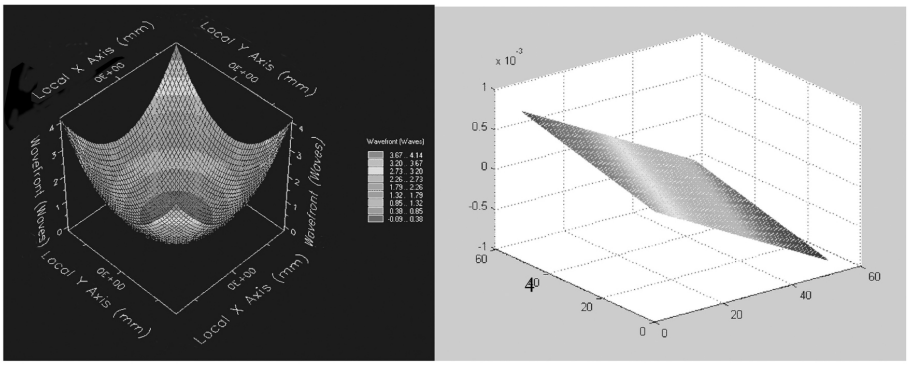

(a) Wavefront distribution (b) Wavefront variation
(a) 波前分布 (b) 波前变化

Fig. 12 Wavefront distribution and variation at 5×10^6 km with X decenter of M2 of 0.5 μm

图 12 次镜 M2 在 X 方向偏心 0.5 μm 时 5×10^6 km 处波前分布和变化量

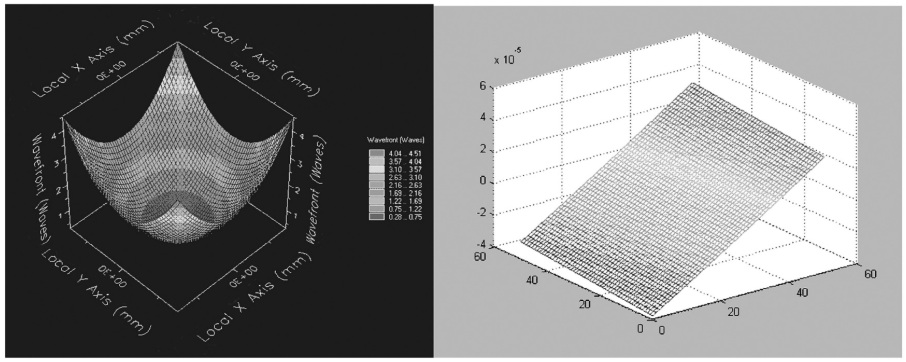

(a) Wavefront distribution (b) Wavefront variation
(a) 波前分布 (b) 波前变化

Fig. 13 Wavefront distribution and variation at 5×10^6 km with Y decenter of M2 of 0.5 μm

图 13 次镜 M2 在 Y 方向偏心 0.5 μm 时 5×10^6 km 处波前分布和变化量

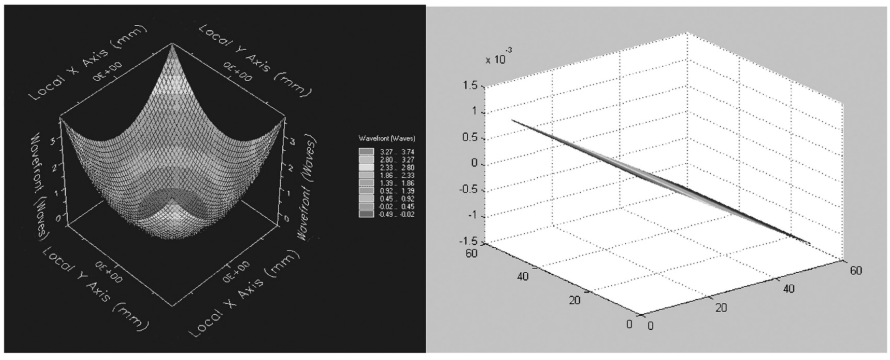

(a) Wavefront distribution (b) Wavefront variation
(a) 波前分布 (b) 波前变化

Fig. 14 Wavefront distribution and variation at 5×10^6 km with Z decenter of M2 of 0.5 μm

图 14 次镜 M2 在 Z 方向偏心 0.5 μm 时 5×10^6 km 处波前分布和变化量

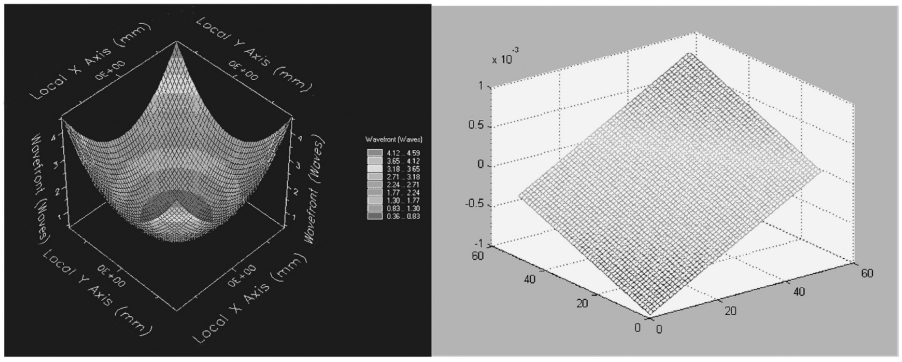

(a) Wavefront distribution　　(b) Wavefront variation
(a) 波前分布　　(b) 波前变化

Fig. 15　Wavefront distribution and variation at 5×10^6 km with M2 rotating around X by $0.4''$

图 15　次镜 M2 绕 X 轴旋转 $0.4''$时 5×10^6 km 处波前分布和变化量

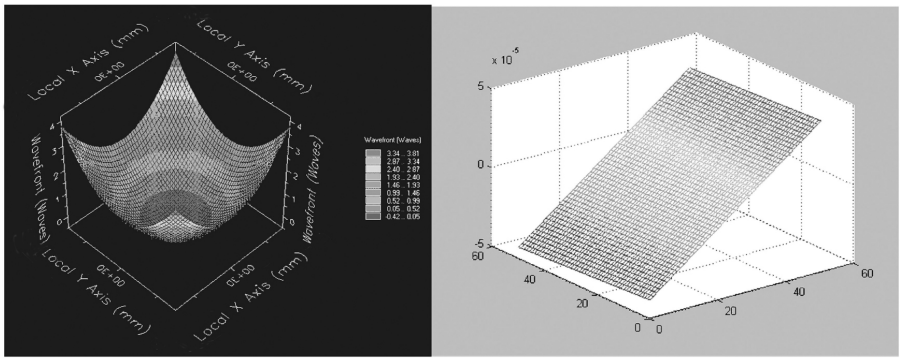

(a) Wavefront distribution　　(b) Wavefront variation
(a) 波前分布　　(b) 波前变化

Fig. 16　Wavefront distribution and variation at 5×10^6 km with M2 rotating around Y by $0.4''$

图 16　次镜 M2 绕 Y 轴旋转 $0.4''$时 5×10^6 km 处波前分布和变化量

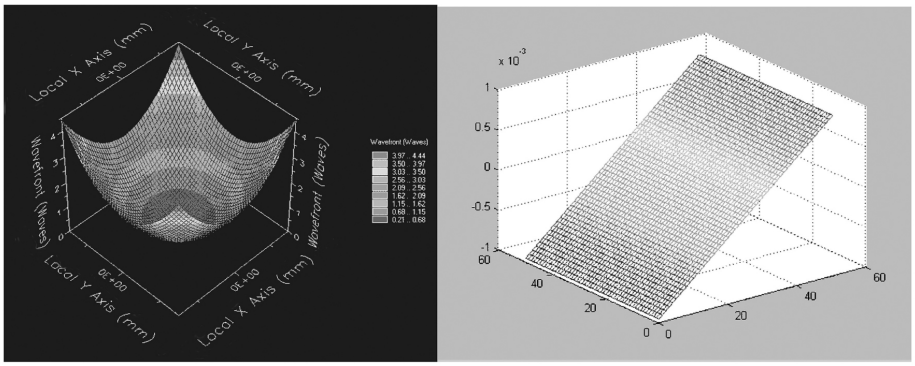

(a) Wavefront distribution　　(b) Wavefront variation
(a) 波前分布　　(b) 波前变化

Fig. 17　Wavefront distribution and variation at 5×10^6 km with M2 rotating around Z by $0.4''$

图 17　次镜 M2 绕 Z 轴旋转 $0.4''$时 5×10^6 km 处波前分布和变化量

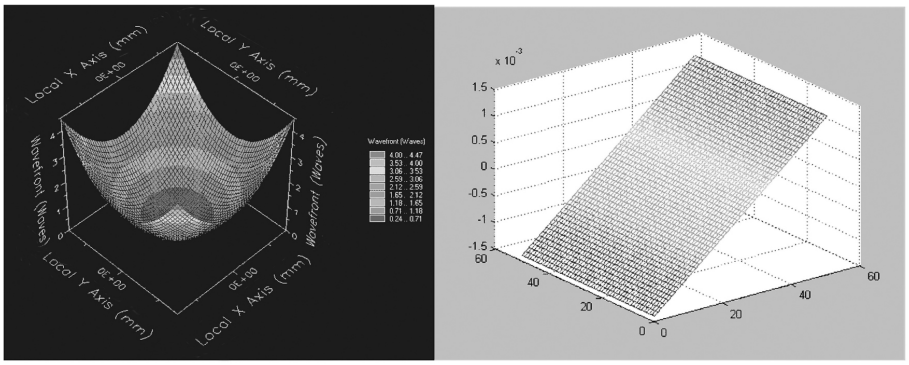

(a) Wavefront distribution
(a) 波前分布

(b) Wavefront variation
(b) 波前变化

Fig. 18 Wavefront distribution and variation at 5×10^6 km with radius change of M2 of 1 μm

图 18 次镜 M2 半径变化 1 μm 时 5×10^6 km 处波前分布和变化量

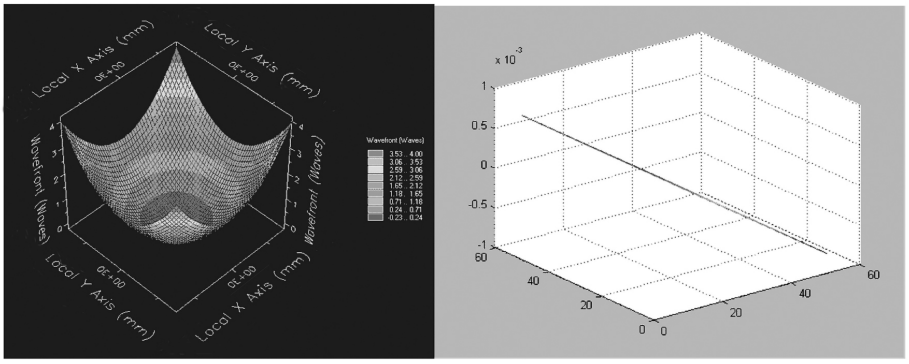

(a) Wavefront distribution
(a) 波前分布

(b) Wavefront variation
(b) 波前变化

Fig. 19 Wavefront distribution and variation at 5×10^6 km with conic change of M2 of 0.001

图 19 次镜 M2 二次曲面系数变化 0.001 时 5×10^6 km 处波前分布和变化量

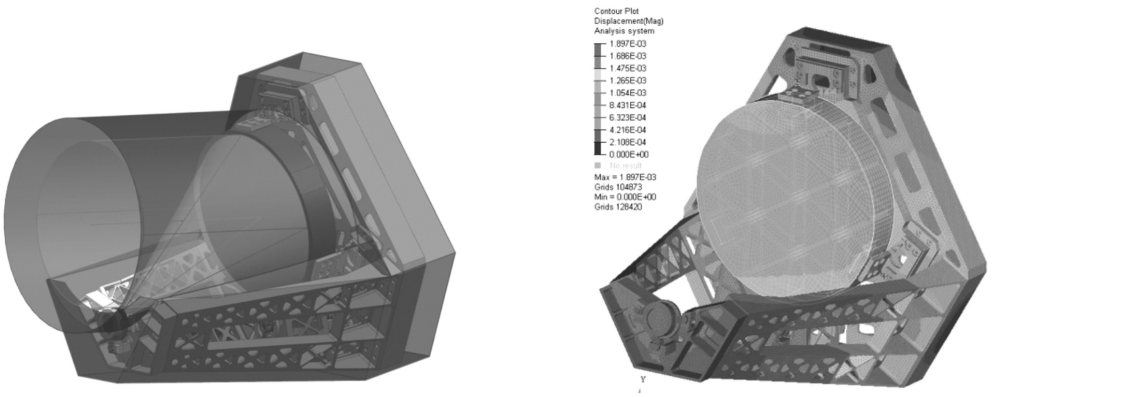

(a) Opto-mechanical design
(a) 光机结构设计

(b) Deformation nephogram caused by in-orbit temperature and gravity release
(b) 在轨温度和重力释放引起结构变形云图

Fig. 20 Telescope prototype

图 20 望远镜原理样机

(3) Integrated opto-mechanical-thermal analysis

光机热集成分析

The principle prototype of the telescope is shown in Fig. 20(a). The reflective mirror is made of grade 0 crystallite and adopts invar which matches the coefficient of linear expansion. Fig. 20(b) is the structural deformation nephogram due to in-orbit temperature and gravity release [15]. Fig. 21 shows the fitting nephogram of the each reflective mirror obtained by the surface fitting. The position change of each mirror is shown in Tab. 4. Returning the surface shape and position of each mirror to the optical system for iteration, the wavefront of each field of view of the telescope is obtained, as shown in Fig. 22.

望远镜原理样机见图 20(a)**,反射镜采用** 0 **级微晶,结构采用匹配线胀系数的殷钢; 图** 20(b) **为在轨温度和重力释放引起的结构变形云图** [15]**。通过面形拟合得到各反射镜的面形云图如图** 21 **所示,各反射镜的位置变化见表** 4**。将各反射镜面形和位置变化返回光学系统进行迭代,得到望远镜各视场的波前,如图** 22 **所示。**

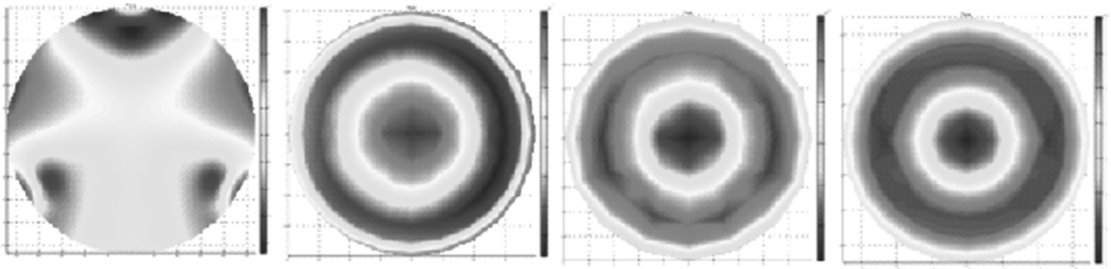

(a) M1　(b) M2　(c) M3　(d) M4

Fig. 21　Surface nephograms of mirrors

图 21　**各反射镜面形云图**

Tab. 4　Translaton and rotation of mirrors

表 4　**各反射镜的平动和转动**

	M1	M2	M3	M4
PV/nm	45.721	1.663	0.121	0.711
RMS/nm	8.927	0.503	0.032	0.183
ΔX/μm	0.001	-0.369	-0.005	-0.024
ΔY/μm	-0.403	0.977	0.497	-1.271
ΔZ/μm	0.855	1.407	0.540	-0.988
$\Delta\theta_x$/(″)	-0.363	-0.009	2.570	2.063
$\Delta\theta_y$/(″)	0.104	-0.403	0.011	0.027

The analysis shows that under the orbital environment, the wavefront of the telescope system changes from $\lambda/60$(RMS) to $\lambda/50$(RMS), which is better than $\lambda/30$(RMS) required for interferometric measurement, so the system wavefront changes caused by the telescope entering the orbital environment from the ground environment meets the requirements of space laser interferometry gravitational wave detection.

经分析,在轨环境下,望远镜系统波前由 $\lambda/60$(RMS) **变化为** $\lambda/50$(RMS)**,优于干涉测量所要求的** $\lambda/30$(RMS)**,所以望远镜从地面环境进入轨道环境引起的系统波前变化满足空间激光干涉引力波探测的需求。**

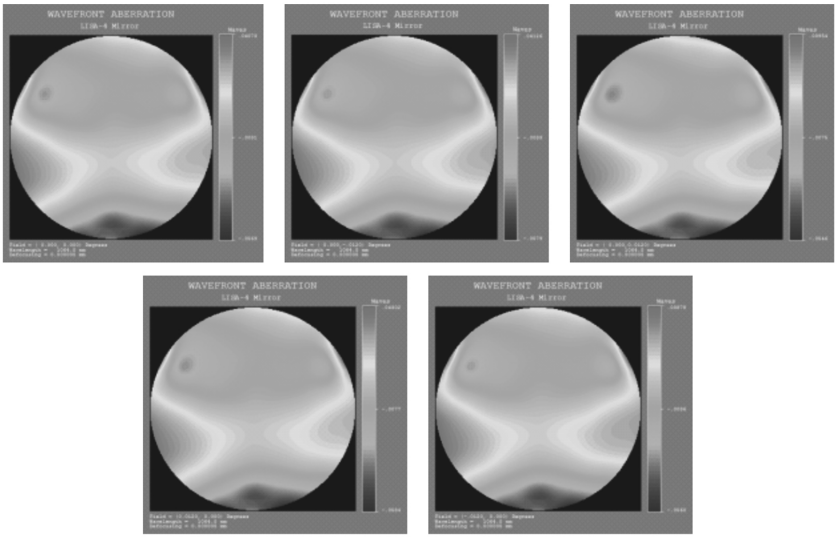

Fig. 22 Wavefront performance of all fields for in-orbit telescope

图 22 在轨望远镜各视场波前

4 Conclusion
结 论

On May 31, 2017, an internal press conference organized by the LIGO and the Virgo Scientific Cooperation Organization confirmed the third gravitational wave event, indicating that the era of gravitational wave astronomy has come. With the return of NASA, the LISA project of the cooperation between Europe and the United States is expected to be launched 5 years ahead of schedule. China's Taiji and Tianqin space gravitational wave detection programs are actively conducting key technological breakthroughs. For this telescope which is a key component of the interferometry measurement system, we hope that we can accomplish key technology research in this kind of telescope as soon as possible and speed up China's space gravitational wave detection program.

2017 年 5 月 31 日,LIGO 和 Virgo 科学合作组织举行的一次内部媒体发布会,确认了第三次引力波事件,表明引力波天文学的时代已经到来。随着 NASA 的回归,欧美合作的 LISA 计划预计提前 5 年发射升空,中国的太极、天琴空间引力波探测计划都在积极地进行关键技术攻关。作为干涉测量系统关键部件的望远镜,希望在进一步分析及原理样机测试的基础上,早日完成关键技术攻关,加速推进我国的空间引力波探测计划。

参考文献:

[1] KARSTEN D. LISA(Unveiling a hidden Universe) Assessment Study Report [R]. ESA/SRE,2011,3.

[2] JEFFREY C L,SHANNON R S. Optical telescope system-level design considerations for a space-based gravitational wave mission [J]. *SPIE*,2011,9904:99041K.

[3] OTTO M. Time-delay interferometry simulations for the laser interferometer space antenna [D]. Hannover: Max Planck Institute for Gravitational Physics,2015.

[4] **罗子人,白姗,边星,等. 空间激光干涉引力波探测 [J]. 力学进展,**2013,43(4):415-447.
LUO Z R,BAI SH,BIAN X,*et al*.. Gravitational wave detection by space laser interferometry [J]. *Advances in Mechanics*, 2013,43(4):415-447. (in Chinese)

[5] **戚子文,刘炳国,张仲海,等. 双点干涉法位相缺陷检测中的解相算法比较 [J]. 中国光学,**2016,9(4):483-490.
QI Z W,LIU B G,ZHANG ZH H,*et al*. Comparison of phase extraction algorithms in testing of phase defects with two-

point interference [J]. *Chinese Optics*,2016,9(4):483-490. (in Chinese)

[6] 王智,马军,李静秋,等. 空间引力波探测计划-LISA 系统设计要点 [J]. 中国光学,2015,8(6):980-987.
WANG ZH,MA Jun,LI J Q,*et al*.. Space-based gravitational wave detection mission: design highlights of LISA system [J]. *Chinese Optics*,2015,8(6):980-987. (in Chinese)

[7] MARCELLO S. Payload preliminary design description [R]. LISA-MSE-DD-0001,Issue 1,rev 1,2009.

[8] OLIVER J. NGO(Revealing a hidden Universe: opening a new chapter of discovery) Assessment Study Report [R]. ESA/SRE(2011)19,December 2011.

[9] BENDER P,BRILLET A. LISA Pre-phase A Report [R]. Max-Planck-Institut for Quantenoptic,1998.

[10] BENDER P L. Wavefront distortion and beam pointing for LISA [J]. *Class. Quantum Grav*,2005,22(S):339-346.

[11] SANKAR S,LIVAS J. Testing and characterization of a prototype telescope for the evolved Laser Interferometer Space Antenna(eLISA) [J]. *SPIE*,9904:99045A.

[12] VERLAAN A L,HOGENHUIS H,PIJNENBUR G J,*et al*.. LISA telescope assembly optical stability characterization for ESA [J]. *SPIE*,2012,8450,845003.

[13] LIVAS J,SANKAR S. Optical telescope design study results [J]. *J. Physics: Conference Series*,2015,610:012029.

[14] 宋同消. 空间引力波探测中激光波前误差分析 [D]. 北京: 首都师范大学,2013.
SONG T X. Analysis of wavefront distortion in detection of gravitational wave in space [D]. Beijing: Capital Normal University,2013. (in Chinese)

[15] 杨帅,沙巍,陈长征,等. 空间相机碳纤维框架的设计与优化 [J]. 光学 精密工程,2017,25(3):697-705.
YANG SH,SHA W,CHEN CH ZH,*et al*.. Design and optimization of carbon fiber framework for space camera [J]. *Opt. Precision Eng*.,2017,25(3):697-705. (in Chinese)

作者简介:

WANG Zhi(1978—), received his Ph. D. degree from Changchun Institute of Optics and Fine Mechanics, Chinese Academy of Sciences in 2006. Currently, Dr. Wang is a visiting scholar at Max Planck Institutein Germany where he is conducting research activities in the areas of space gravitational wave detection. E-mail: wz070611@126.com

王　智(1978—),男,山东寿光人,博士,研究员,2003 年于长春理工大学获得硕士学位,2006 年于中科院长春光机所获得博士学位,现为德国马普爱因斯坦研究所访问学者,主要从事空间引力波探测方面的研究。E-mail: wz070611@126.com